RESEARCH   **Open Access**

Tailoring pullulanase PulAR from *Anoxybacillus* sp. AR-29 for enhanced catalytic performance by a structure-guided consensus approach

Shu-Fang Li[1,2,3], Shen-Yuan Xu[1,2,3], Ya-Jun Wang[1,2,3]* and Yu-Guo Zheng[1,2,3]

Abstract

Pullulanase is a well-known debranching enzyme that can specifically hydrolyze α-1,6-glycosidic linkages in starch and oligosaccharides, however, it suffers from low stability and catalytic efficiency under industrial conditions. In the present study, four residues (A365, V401, H499, and T504) lining the catalytic pocket of *Anoxybacillus* sp. AR-29 pullulanase (PulAR) were selected for site-directed mutagenesis (SDM) by using a structure-guided consensus approach. Five beneficial mutants (PulAR-A365V, PulAR-V401C, PulAR-A365/V401C, PulAR-A365V/V401C/T504V, and PulAR-A365V/V401C/T504V/H499A) were created, which showed enhanced thermostability, pH stability, and catalytic efficiency. Among them, the quadruple mutant PulAR-A365V/V401C/T504V/H499A displayed 6.6- and 9.6-fold higher catalytic efficiency toward pullulan at 60 ℃, pH 6.0 and 5.0, respectively. In addition, its thermostabilities at 60 ℃ and 65 ℃ were improved by 2.6- and 3.1-fold, respectively, compared to those of the wild-type (WT). Meanwhile, its pH stabilities at pH 4.5 and 5.0 were 1.6- and 1.8-fold higher than those of WT, respectively. In summary, the catalytic performance of PulAR was significantly enhanced by a structure-guided consensus approach. The resultant quadruple mutant PulAR-A365V/V401C/T504V/H499A demonstrated potential applications in the starch industry.

Keywords: Pullulanase, Structure-guided consensus approach, Site-directed mutagenesis, Catalytic pocket, Stability, Catalytic efficiency

*Correspondence: wangyj@zjut.edu.cn; yajun246@hotmail.com
[1] Key Laboratory of Bioorganic Synthesis of Zhejiang Province, College of Biotechnology and Bioengineering, Zhejiang University of Technology, 18 Chaowang Road, Hangzhou 310014, People's Republic of China
Full list of author information is available at the end of the article

Li *et al. Bioresources and Bioprocessing*   (2022) 9:25

Page 2 of 11

Graphical Abstract
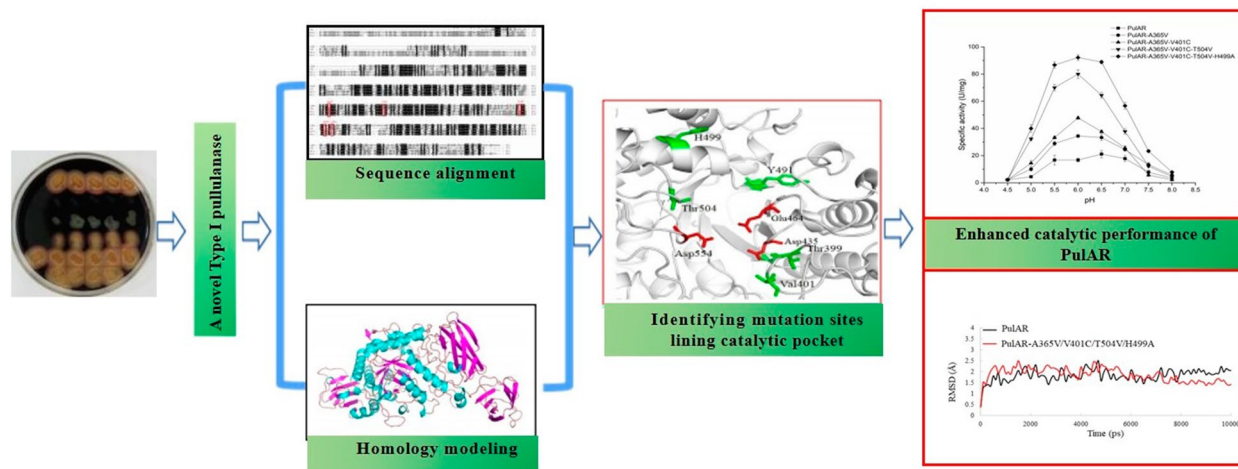
Introduction

Starch transformation can be accomplished by using an enzymatic process that involves two primary steps: liquefaction and saccharification (Hii et al. 2012). Generally, the saccharification is conducted at 60 °C and pH 4.5–5.5 for 48–60 h, via pullulanase in combination with β-amylase or glucoamylase, producing maltose syrup and glucose syrup. Pullulanase [EC 3.2.1.41] is a debranching enzyme that can specifically cleave α-1,6-glycosidic linkages in pullulan, starch, amylopectin, glycogen, and related oligosaccharides (Bertoldo and Antranikian 2002). Addition of pullulanase would reduce the amount of glucoamylase or β-amylase used in the saccharification step and improve substrate concentration and conversion (Duan et al. 2013). High-purity maltose syrup is a low-calorie, low-sweetness sugar that is being widely used in the food, medicine, and cosmetic industries (Bertoldo et al. 1999), in which the content of maltose is above 60%. In recent years, enzymatic preparation of maltose syrups has drawn rising interest for its mild reaction condition, high selectivity, and high catalytic efficiency (Lin et al. 2013). In combination with β-amylase and/or maltase, pullulanase can raise starch hydrolysis efficiency to high-purity maltose syrup and reduce production cost.

Pullulanases are divided into type I pullulanase and type II pullulanase based on substrate specificity and reaction products. Type II pullulanase hydrolyzes both α-1,6-glycosidic linkages and α-1,4-glycosidic linkages (Kang et al. 2011; Li et al. 2012; Pang et al. 2019). Compared with type II pullulanase, type I pullulanase specifically hydrolyzes α-1,6-glycosidic linkages in pullulan and other polysaccharides, forming maltotriose and linear oligomers. In recent years, a few type I pullulanases from *Fervidobacterium nodosum* Rt17-B1(Yang et al. 2020), *Bacillus methanolicus* PB1 (Zhang et al. 2020), *Geobacillus thermocatenulatus* DSMZ73010 (Li et al. 2018), *Bacillus megaterium* W1210 (Yang et al. 2017), *Anoxybacillus* sp. SK3-4 (Kahar et al. 2016) and *Paenibacillus polymyxa* Nws-pp2 (Wei et al. 2015) have been cloned and characterized. However, most of the reported type I pullulanases exhibit neutral or basic pH optimum, and their stabilities under acidic or thermophilic conditions are usually poor.

Protein engineering is an efficient way to obtain the desirable enzymes (Böttcher and Bornscheuer 2010). As reported previously, many reports focused on enhancing the thermostability or catalytic efficiency of the type I pullulanases. For example, Duan et al. successfully improved the thermostability and catalytic efficiency of a Type I pullulanase from *Bacillus deramificans* by site-directed mutagenesis (SDM) (Duan et al. 2013). In a recent example, Bi and coworkers employed a computer-aided method to raise *Tm* of the thermophilic pullulanase from *Bacillus thermoleovorans* by 3.8 °C (Bi et al. 2020). Up to date, only a limited number of reports on improving acidic adaptation of pullulanase are available (Wang et al. 2017; Zeng et al. 2019). Chen and coworkers improved the acidic adaptation of *Bacillus acidopullulyticus* pullulanase by altering hydrogen bonds network near the catalytic residues, shifting its optimum pH from 5.0 to 4.0 at the expense of activity reduction (Chen et al. 2019). Therefore, it is still needed to dig out the pullulanase with high catalytic efficiency and stability under thermophilic and acidic conditions.

Li *et al. Bioresources and Bioprocessing*   (2022) 9:25

Page 3 of 11

In this study, we identified a novel pullulanase from *Anoxybacillus* sp. AR-29 (PulAR). Four residues A365, V401, H499, and T504 lining the catalytic pocket were identified as critical for the thermostability and acid resistance by a structure-guided consensus approach. The catalytic performance of PulAR under thermophilic and acidic conditions was enhanced by SDM. In addition, structural analysis and MD simulations were performed to elucidate their roles.

Materials and methods

Bacterial strains, plasmids, and enzyme

The *Anoxybacillus* sp. AR-29 strain was isolated and stored in our laboratory. The PulAR gene (GenBank accession number KY273924.1) was cloned from *Anoxybacillus* sp. AR-29. We have constructed the pET-32a (+)-*PulAR* plasmid in our previous study. *Escherichia coli* DH5α was used as the host for the cloning work, and *E. coli* BL21(DE3) was the host for the expression of the enzymes. Phanta Super-Fidelity DNA Polymerase and the restriction enzyme *Dpn* I were purchased from Vazyme Biotech Co., Ltd (Nanjing, China). All other chemicals and reagents were obtained from standard commercial sources.

Genomic DNA extraction, amplification and bioinformatics analysis

The genomic DNA of *Anoxybacillus* sp. AR-29 was extracted using TIANamp Bacteria DNA Kit (Tiangen, Beijing, China). And the genomic DNA of *Anoxybacillus* sp. AR-29 was used as the template for the amplification of the pulAR-encoding gene, using the forward primer 5′-GCGATATCATGTATGAGGTCTTTTCC-3′ and reverse primer 5′-GCCTCGAGTTATATGTGATTTGCTTTTT-3′, respectively. *PulAR* gene was amplified by PCR according to the following protocol: denaturation at 95 °C for 60 s, 20 cycles of (95 °C, 30 s; 55 °C, 30 s; 72 °C, 90 s), and a final extension at 72 °C for 10 min. The protein sequence and nucleotide sequence of PulAR were analyzed by using BLASTp and BLASTn (http://www.ncbi.nlm.nih.gov/), respectively. The MW and pI of this enzyme were predicted via the web server (http://web.expasy.org/compute_pi/).

Cloning, over-expression and purification of PulAR

The PCR products were double digested with the restriction enzymes *EcoR* V and *Xho* I and cloned into the pET-32a (+), which was also digested by the same restriction enzymes, yielding the recombinant plasmid pET-32a (+)-*PulAR.* For over-expression of PulAR in *E. coli* BL21(DE3), the recombinant plasmid was transformed into *E. coli* BL21(DE3). The transformant was picked into the tube with 5 mL LB medium containing 100 µg/mL

ampicillin and cultivated at 37 °C overnight. The overnight cultures were then transferred into another 100 mL of LB medium containing ampicillin (100 µg/mL), and cultivated for 3 h until the OD at 600 nm was between 0.6 and 0.8. The protein expression was then induced by adding IPTG at a final concentration of 0.5 mM for 16 h at 16 °C. The cells were harvested by centrifugation at 8000*g* for 10 min at 4 °C and resuspended in 20 mL of binding buffer (20 mM Tris–HCl, 250 mM NaCl, 20 mM imidazole). Cell lysates were prepared with a French press operating at 4 °C, and then centrifuged at 8000*g* for 30 min. The resultant soluble fraction was micro-filtrated, and loaded onto a Ni–NTA column which was pre-equilibrated with the binding buffer. The target protein was eluted by a 20–250 mM imidazole gradient at a flow rate of 1 mL/min. The protein was pooled and dialysed with Buffer C (20 mM Tris–HCl and 150 mM NaCl, pH 8.0). The purified protein was estimated by SDS-PAGE, and the concentration of the protein was determined by the BCA protein assay kit.

Characterization of WT-PulAR

Pullulanase activity was measured in 500 µL reaction mixtures that contained 50 µL of pullulan (0.5%), 400 µL of sodium phosphate buffer (100 mM, pH 6.0), and the appropriate amounts of the purified enzymes, and incubated at 60 °C for 10 min. One unit of pullulanase activity was defined as the amount of enzyme required to release 1 µmol of reducing sugars per minute. Effects of pH on the purified PulAR were determined in 100 mM buffer over pH 3.6–9, including sodium acetate buffer (pH 3.6–5.8), sodium phosphate buffer (pH 5.8–7.5) and Tris–HCl buffer (pH 7.5–9.0). The temperature optimum of PulAR was measured at temperatures between 45 and 95 °C in 100 mM sodium acetate buffer (pH 6.0).

The kinetic parameters of WT-PulAR were determined according to the method as previously described (Li et al. 2015), using pullulan at varying concentrations (1.0, 1.25, 1.33, 2.0, 2.5, 3.33, and 5.0 mg/mL) as substrate at 60 °C for 10 min in 100 mM buffer (pH 6.0). Experiments were conducted in triplicates. The Michaelis–Menten equation was fitted to the data points to determine K_M and v_{max} by nonlinear least-squares regression analysis using Origin 8.5.

Screening for hotspot residues by a structure-guided consensus approach

The protein sequence of PulAR was aligned with the pullulanases from *Anoxybacillus* sp. 18–11 (pH$_{opt}$ 6.0) (PulA) (Xu et al. 2014), *Bacillus acidopullulyticus* (pH$_{opt}$ 5.0) (*Ba*pul) (Turkenburg et al. 2009), and *Bacillus naganoensis* (pH$_{opt}$ 4.5) (*Bn*pul) (Nie et al. 2013). The temperature optimum range of these pullulanases was 55–65 °C. The

Li *et al. Bioresources and Bioprocessing*   (2022) 9:25

Page 4 of 11

putative structure of PulAR was obtained with the homology-modeling pipeline SWISS-MODEL server (http://swiss-model.expasy.org), using the structure of type I pullulanase (PDB ID: 3WDH) from *Anoxybacillus* sp. LM18-11 as the template. The structures were analyzed and visualized by using PyMOL (http://www.pymol.org/). The residues within 8 Å of the catalytic triad of PulAR were identified and the differences in these amino acid residues among the above pullulanases were explored. Totally, five residues (A365, T399, V401, Y491, and T504) different from those of the acidophilic pullulanases (*Ba*pul and *Bn*pul) were selected for SDM. In addition, the mutation Y477A could improve the thermostability of a Type I pullulanase PulA in our previous report (Li et al. 2015). Therefore, the residue H499 of PulAR was also chosen for SDM, which was corresponding to Y477 of PulA.

Construction of the mutants

The PulAR gene was cloned into the pET-32a(+) plasmid, and the recombinant plasmid pET-32a(+)-*PulAR* was used as the template for site-directed mutagenesis. The PCR was conducted as follows: 95 °C for 5 min, then 26 cycles (95 °C for 30 s, 50 °C for 30 s, and 72 °C for 8 min), and final extension at 72 °C for 10 min. The PCR reaction system (25 μL) consisted of 12.5 μL 2 × Phanta buffer, 0.5 μL dNTP mixture (each at 10 mmol L^{-1}), 1 μL forward primer (10 μmol L^{-1}), 1 μL reverse primer (10 μmol L^{-1}), 1 μL plasmid template (50 ng), 8.5 μL ultra-pure water, and 0.5 μL DNA polymerase (1 U μL^{-1}). The primers are listed in Additional file 1: Table S1. The PCR products were digested with *Dpn* I and then transformed into *E. coli* BL21(DE3). To verify that only the designated mutations were inserted by the DNA polymerase, the full plasmids containing the pullulanase gene were sequenced.

Expression, purification and characterization of PulAR mutants

Expression, purification, and characterization of the PulAR mutants were conducted according to the methods described above as 2.3 and 2.4. The purified protein was analyzed by SDS-PAGE (Additional file 1: Fig. S1).

Structural and MD simulation analyses of PulAR

Homology modeling of the PulAR mutants was performed with the same approach as used for WT. Discovery Studio and DSSP web server (http://www.cmbi.ru.nl/xssp/) were adopted to analyze the structural information. YASARA software was used for molecular dynamics simulation (MD simulation). MD simulations were performed at 60 °C and pH 5.0 for 20 ns. During the dynamic simulation, the force field was Amber 03, the TIP3P model was used, and the concentration

of NaCl was set at 0.9%. After initial minimization through the steepest descent and simulated annealing, convergence was reached. The time step is 1 fs, and the track is saved every 100 ps. All independent MD simulations were repeated three times.

Results and discussion

Sequence analysis of PulAR encoding gene

The pullulanase PulAR gene (2,259 bp long, GenBank accession number KY273924.1) has a putative translational start site GTG with a G + C content of 78.4%, and encodes an enzyme with a predicted molecular mass of 85.0 kDa with a theoretical pI of 5.49. The structure of PulAR was constructed based on the crystal structure of the pullulanase PulA from *Anoxybacillus* sp. LM18-11 (PDB ID: 3WDH), with which it shares 58.29% identity (Fig. 1A). Analysis of the protein sequence of PulAR by NCBI BLASTp showed that it contains the YNW-GYDP motif and four conserved regions (I–IV) (Additional file 1: Fig. S2), which are similar to those of type I pullulanases and comprise a catalytic triad and several substrate binding sites. Therefore, the residues D435, E464, and D554 of PulAR are inferred as the catalytic residues. No signal peptide was found in the pullulanase PulAR through analysis by Signal P (https://services.healthtech.dtu.dk/service.php?SignalP-4.1). Comparison with the pullulanase sequences in the GenBank database, listed in Table 1, revealed that PulAR shares 70.8%, 60.2%, 58.3%, 46.5%, 43.6%, 41.5%, 41.1% and 38.1% identity with the thermostable pullulanases from *Bacillus stearothermophilus* (Kuriki et al. 1990), *Geobacillus thermoleovorans* (Zouari Ayadi et al. 2008), *Anoxybacillus* sp. LM18-11 (Xu et al. 2014), *Bacillus* sp. CICIM 263 (Li et al. 2012), *Anaerobranca gottschalkii* (Bertoldo et al. 2004), *Fervidobacterium pennivorans* DSM 9078 (Bertoldo et al. 1999), *Thermotoga neapolitana* (Kang et al. 2011), and *Caldicellulosiruptor saccharolyticus* (Albertson et al. 1997), respectively.

Screening for mutation hotspots

To identify the critical residues responsible for catalytic activity and stability of PulAR, we compared the protein sequences of neutrophilic type I pullulanases (PulA and PulAR) with the acidophilic pullulanases (*Bn*Pul and *Ba*Pul) (Fig. 1a), which have temperature and pH optima of 50–60 °C and pH 4.5–6.0. The differences in the amino acid residues among the above pullulanases within 8 Å of the catalytic triad were explored (Fig. 1b), and six mutants A365V, T399S, V401T, V401C, Y491V, and T504V, were generated. Besides, the single mutant H499A was also constructed.
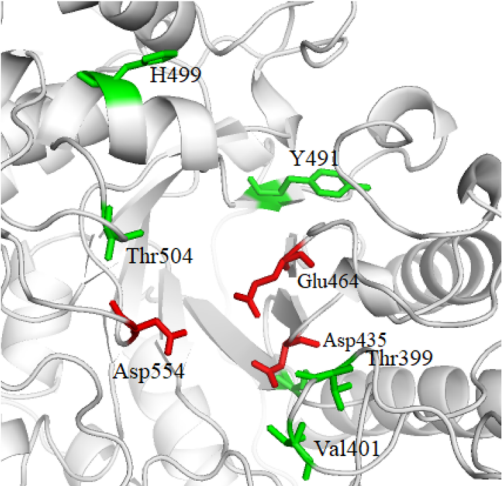
Li *et al. Bioresources and Bioprocessing*   (2022) 9:25

Page 5 of 11

(a)
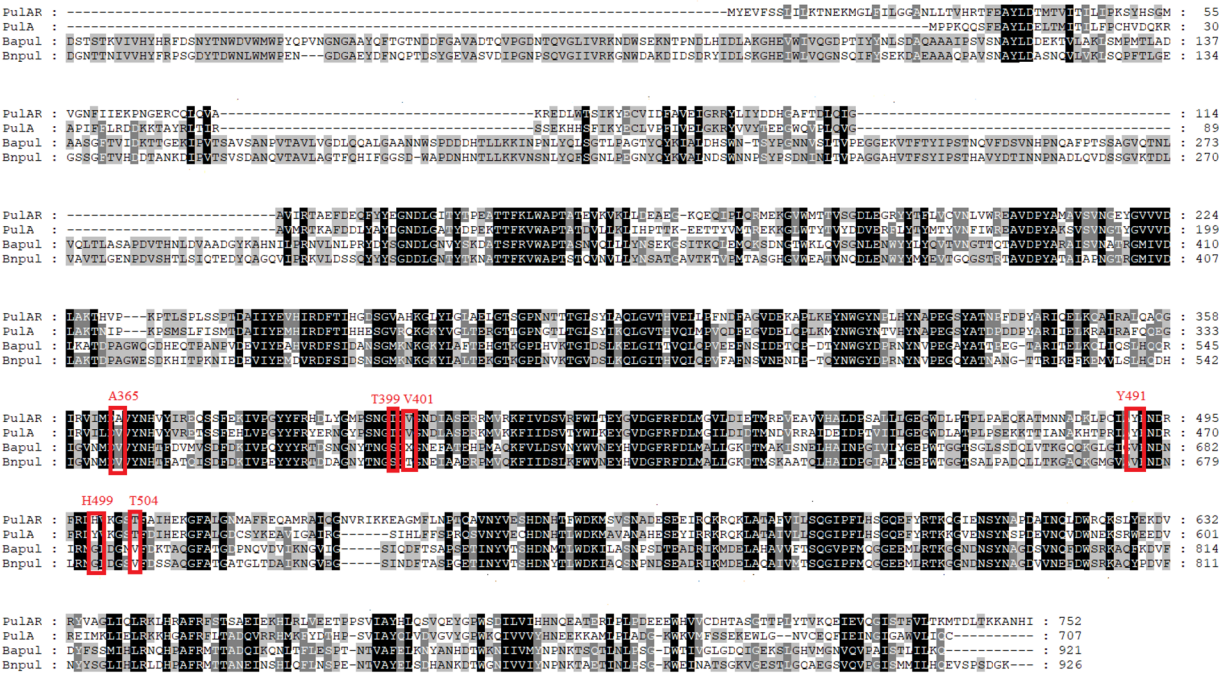
(b)

Fig. 1 **a** Sequence alignment of PulAR with *Bacillus acidopullulyticus* pullulanase (*Ba*pul) and *Bacillus naganoensis* pullulanase (*Bn*pul). **b** Mutation hotspots A365, T399, V401, Y491, and T504

Li *et al. Bioresources and Bioprocessing*   (2022) 9:25

Page 6 of 11

Table 1 Comparison of optimum temperatures between bacterial type I pullulanases

Bacterial source	Accession number	Optimum temperature (℃)	Similarity with PulAR	Special activity	References
Bacillus stearothermophilus	1808262A	60	70.8%	0.214 U/mL	Kuriki et al. ([1990](#))
Geobacillus thermoleovorans	CAC85704.1	70	60.2%	36 U/mg	Zouari Ayadi et al. ([2008](#))
Anoxybacillus sp. LM18-11	AEW23439.1	60	58.3%	v_{max} 750 U/mg	Xu et al. ([2014](#))
Bacillus sp. CICIM 263	AGA03915.1	70	46.5%	73 U/mg	Li et al. ([2012](#))
Anaerobranca gottschalkii	AAS47565.1	65–70	43.6%	56 U/mg	Bertoldo et al. ([2004](#))
Fervidobacterium pennivorans DSM 9078	AAD30387.1	80	41.5%	78 U/mg	Bertoldo et al. ([1999](#))
Thermotoga neapolitana	ACN58254.1	80–85	41.1%	25.1 U/mg	Kang et al. ([2011](#))
Caldicellulosiruptor saccharolyticus	AAB06264.1	85	38.1%	–	Albertson et al. ([1997](#))
Anoxybacillus sp. AR-2	KY273924	55	100.0%	24.4 U/mg	This study
	KY273924	65	99.0%	87.8U/mg (PulAR-A365V/ V401C/T504V/H499A)	This study

Generation of PulAR-positive mutants and enzymatic characterization

Firstly, the pullulanase activities of seven mutants were assayed at pH 5.0 and pH 6.0, respectively, and then the activity ratio of WT and its mutants at pH 5.0 to that at pH 6.0 ($A_{pH5.0}/A_{pH6.0}$) were evaluated. As described in Additional file [1](#): Table S2, $A_{pH5.0}/A_{pH6.0}$ of WT-PulAR and its mutants (A365V, T399S, V401T, V401C, Y491V, T504V and H499A) were 0.20, 0.49, 0.12, 0, 0.75, 0.19, 0.29 and 0.50, respectively. Therefore, we combined the positive mutations A365V, V401C, T504V, and H499A, generating three triple mutants PulAR-A365V-V401C, PulAR-A365V-V401C-T504V, and PulAR-A365V-V401C-T504V-H499A.

We characterized the three combined mutants PulAR-A365V-V401C, PulAR-A365V-V401C-T504V, and PulAR-A365V-V401C-T504V-H499A, as well as two single mutants PulAR-A365V and PulAR-V401C. As shown in Fig. [2](#), the optimum temperature (T_{opt}) of PulAR was 55 ℃, and these of the mutants PulAR-A365V, PulAR-V401C, PulAR-A365V-V401C, PulAR-A365V-V401C-T504V, and PulAR-A365V-V401C-T504V-H499A were 55, 60, 60, 60, and 65 ℃, respectively. Compared with WT, the T_{opt} of the mutant PulAR-A365V-V401C-T504V-H499A was increased by 10 ℃. In addition, at 60 ℃ and pH 6.0, the specific activities of WT and its mutants PulAR-A365V, PulAR-V401C, PulAR-A365V-V401C, PulAR-A365V-V401C-T504V, and PulAR-V401C-T504V-H499A were 24.4, 37.8, 43.3, 48.9, 68.9, and 87.8 U/mg. The optimum pH of PulAR-A365V, PulAR-V401C, PulAR-A365V-V401C, and PulAR-A365V-V401C-T504V was 6.0, which was similar to that of the WT. At 60 ℃ and pH 5.0, the specific activities of PulAR and its mutants

PulAR-A365V, PulAR-V401C, PulAR-A365V-V401C, PulAR-A365V-V401C-T504V, and PulAR-A365V-V401C-T504V-H499A were 4.4, 10.0, 14.4, 32.2, and 40.0 U/mg, respectively. Among them, the specific activity of the quadruple mutant PulAR-A365V-V401C-T504V-H499A was 8.1-fold higher than that of WT at 60 ℃, pH 5.0.

To evaluate the thermostabilities of PulAR and its mutants, the enzymes were incubated at 60 ℃ and pH 6.0, and then the residual activities were assayed after varying incubation times. As shown in Table [2](#), all the mutants PulAR-A365V, PulAR-V401C, PulAR-A365V-V401C, PulAR-A365V-V401C-T504V, and PulAR-A365V-V401C-T504V-H499A displayed increased half-lives. At 60 and 65 ℃, the half-lives ($t_{1/2}$) of PulAR were only 4.8 and 2.5 h, respectively, whereas those of the quadruple mutant were 17.5 and 10.3 h, which were 2.65 and 3.12-fold higher than those of PulAR, respectively. The stabilities of PulAR under the acidic conditions (pH 4.5 and 5.0) were also significantly enhanced. The half-lives of PulAR were 5.4 and 6.1 h at pH 4.5 and 5.0, respectively, whereas those of the quadruple mutant PulAR-A365V-V401C-T504V-H499A displayed longer half-lives of 13.9 and 17.3 h, respectively (Table [3](#)). The structures of PulAR and its mutants were modeled to investigate the mechanisms of the enhanced thermostability and pH stability. Ala365 is buried in the internal of the protein. As shown in Fig. [3](#), the mutation A365V introduces two extra hydrophobic interactions F432-V365 and F434-V365 while maintaining the two hydrogen bonds V365-R433 and D435-V365. The residue V401 is located on the protein surface. The mutation V401C increased the hydrophilicity of the protein surface (Fig. [4](#)), contributing to enhanced thermostability (Yu et al. [2012](#)). Similar to the mutation Y477A in
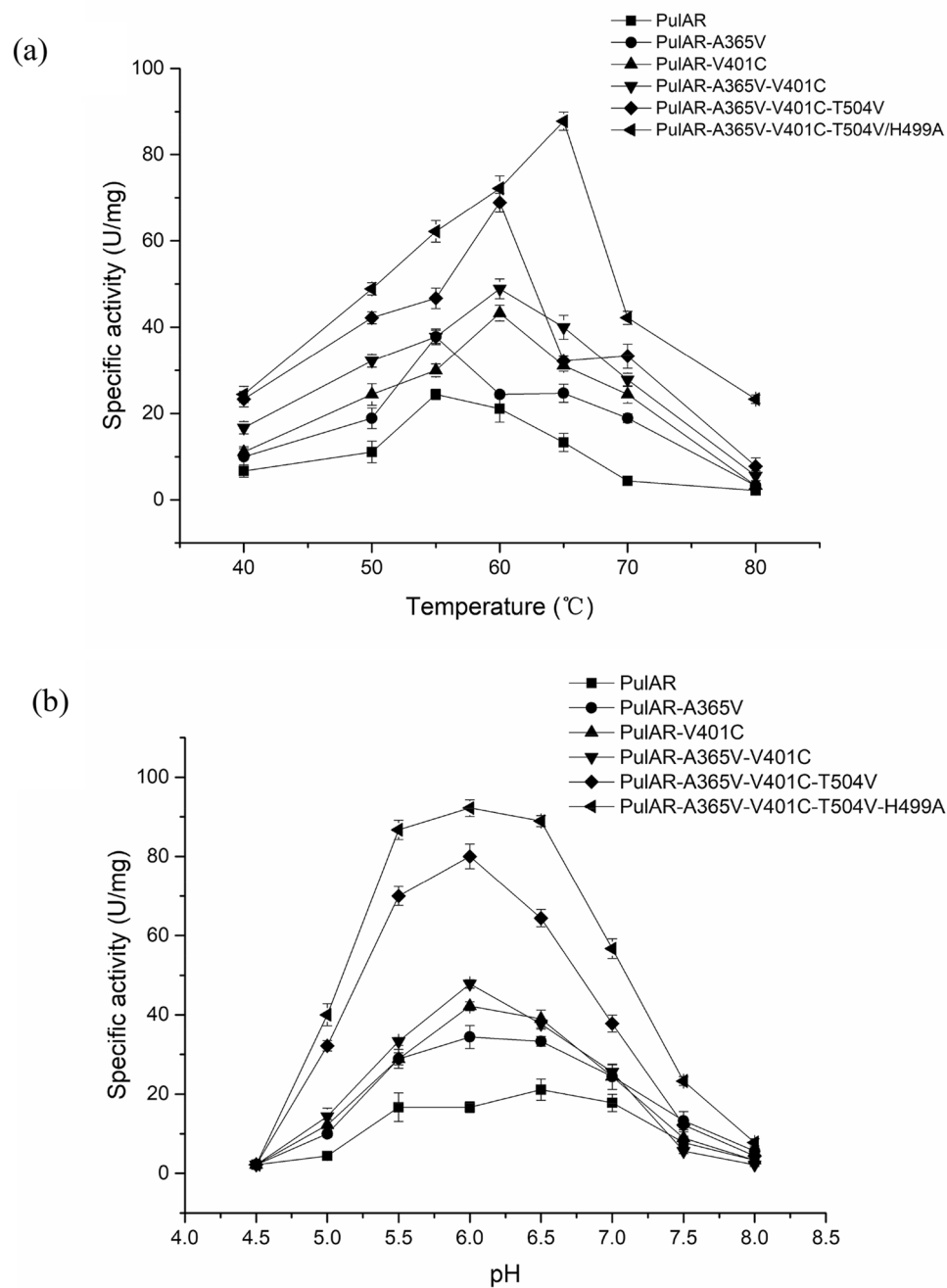
Fig. 2 Temperature (**a**) and pH (**b**) optima of WT-PulAR and its mutants

our previous report, the solvent accessibility of the residue at the position 499 was reduced from 29.9 to 2.4 as assayed by the DSSP web server, which might enable the protein structure of PulAR more compact (Li et al. 2005, 2015). Replacing T504 with Val possessing an extra CH_3 group reinforces the hydrophobic interior of the structure, leading to enhancement of the thermostability and pH stability (Tai et al. 2011).

Li *et al. Bioresources and Bioprocessing*   (2022) 9:25

Page 8 of 11

Table 2 Half-lives of WT-PulAR and its variants at 6065 °C and 65 °C

Mutant	60 °C		65 °C	
	k_d (1/h)	$t_{1/2}$ (h)	k_d (1/h)	$t_{1/2}$ (h)
WT-PulAR	0.14	4.8 ± 0.2	0.28	2.5 ± 0.1
PulAR-A365V	0.12	5.9 ± 0.5	0.17	4.1 ± 0.2
PulAR-V401C	0.12	6.0 ± 0.1	0.17	4.1 ± 0.1
PulAR-A365V-V401C	0.07	9.9 ± 0.2	0.10	6.7 ± 0.4
PulAR-A365V-V401C-T504V	0.05	13.2 ± 0.1	0.08	9.2 ± 0.2
PulAR-A365V-V401C-T504V-H499A	0.04	17.5 ± 0.1	0.07	10.3 ± 0.3

Table 3 Half-lives of WT-PulAR and its variants at pH 4.5 and 5.0

Mutant	pH 4.5		pH5.0	
	k_d (1/h)	$t_{1/2}$ (h)	k_d (1/h)	$t_{1/2}$ (h)
WT-PulAR	0.13	5.4 ± 0.3	0.11	6.1 ± 0.5
PulAR-A365V	0.10	7.0 ± 0.4	0.08	8.5 ± 1.4
PulAR-V401C	0.10	7.1 ± 0.6	0.08	8.4 ± 0.3
PulAR-A365V-V401C	0.07	9.4 ± 0.3	0.06	10.8 ± 0.2
PulAR-A365V-V401C-T504V	0.06	11.1 ± 0.4	0.05	13.6 ± 1.0
PulAR-A365V-V401C-T504V-H499A	0.05	13.9 ± 1.2	0.04	17.3 ± 1.2

Catalytic efficiency measurement and MD analysis

WT-PulAR and its mutants were subjected to kinetic analysis at 60 ℃, pH 5.0 and 6.0, respectively. Compared with WT, at pH 6.0, 60 °C, the K_M values of PulAR-A365V, PulAR-V401C, PulAR-A365V-V401C, PulAR-A365V-V401C-T504V, and PulAR-A365V-V401C-T504V-H499A decreased by 7.3%, 7.3%, 24.4%, 33.5%, and 53.0%, respectively, while the k_{cat} values increased by 39.1%, 54.3%, 168.9%, 193.7%, and 254.3%, respectively (Table 4). In addition, at pH 5.0, 60 °C, the K_M values of PulAR-A365V, PulAR-V401C, PulAR-A365V-V401C, PulAR-A365V-V401C-T504V, and PulAR-A365V-V401C-T504V-H499A decreased by 15.2%, 19.3%, 31.7%, 43.7%, and 68.5%, respectively, while the k_{cat} values increased by 37.7%, 45.7%, 154.8% 196.7%, and 230.7%, respectively (Table 5). Resultantly, the catalytic efficiencies (k_{cat}/K_M) of the "best" quadruple mutant PulAR-A365V-V/V-H499A were 6.6- and 9.6-fold higher than those of PulAR, at pH 6.0 and 5.0, respectively. The catalytic efficiency of PulAR was enhanced by mutations, which were identified by sequence alignment of the acidophilic pullulanase and neutrophilic pullulanase. Further, the roles of A365, V401, T504, and H499 in the structure–function relationship were analyzed. A365, V401, T504 and H499 form the catalytic pocket, shown in Fig. 1b. They are located within 8 Å of the catalytic residues D435, E464,
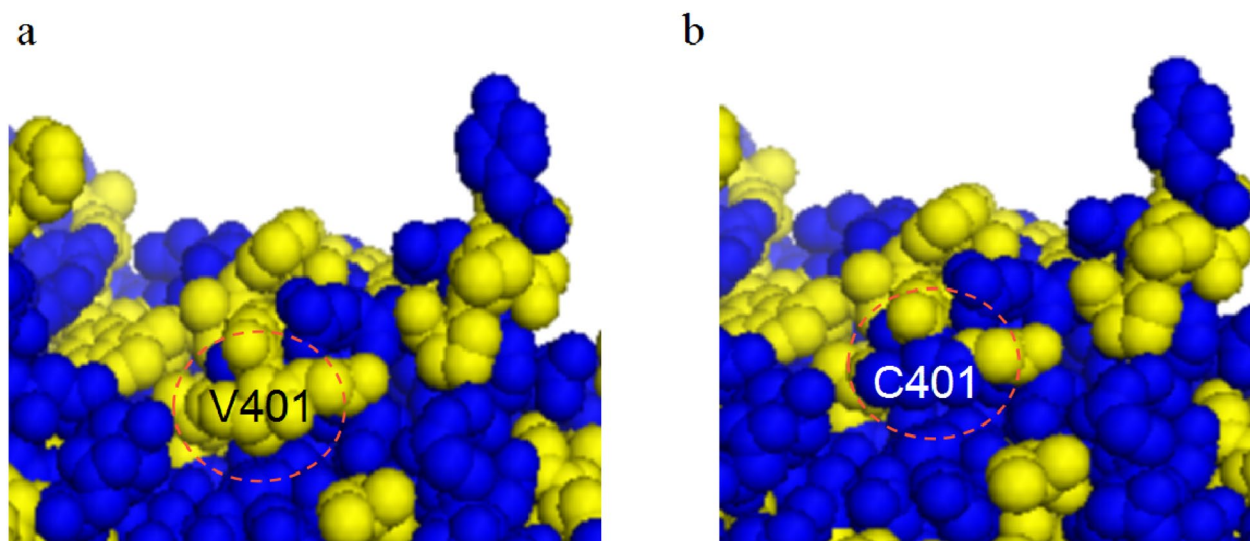

Fig. 3 Structural analysis of PulAR before (**a**) and after (**b**) mutation A365V
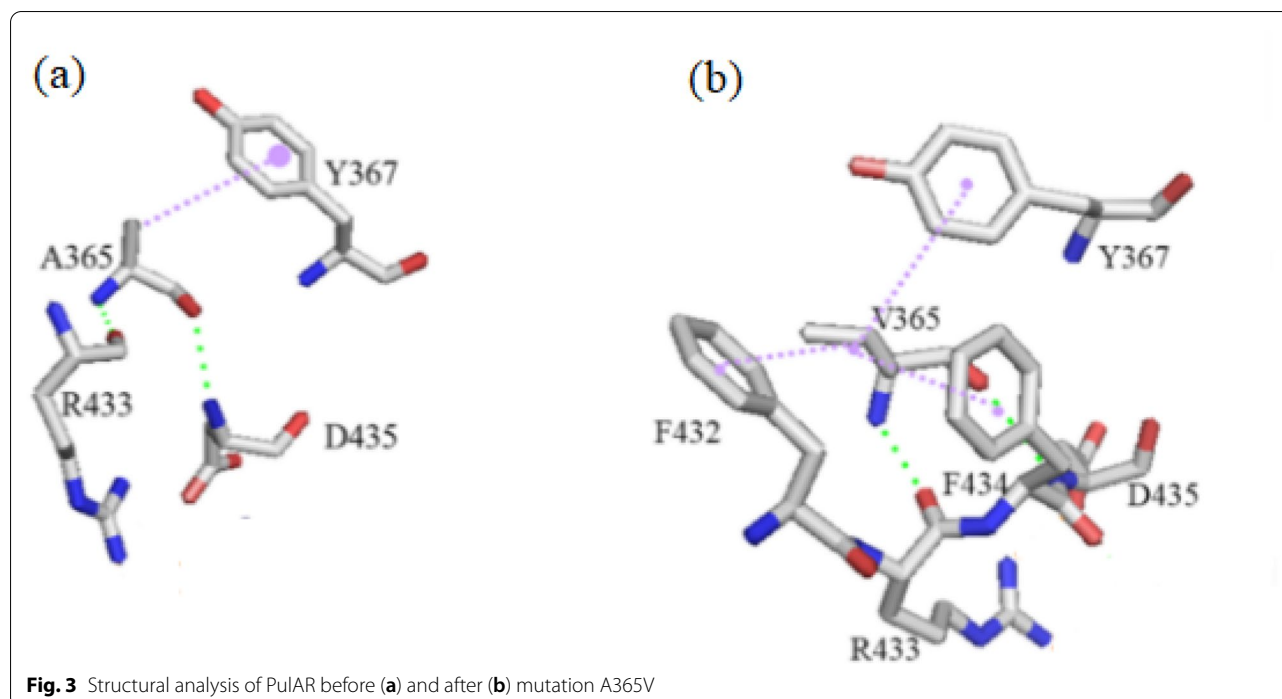
Fig. 4 The hydrophobic residue V401 is shown in yellow (**a**) and the hydrophilic residue C401 is shown in blue (**b**)

Table 4 Catalytic efficiencies of WT-PulAR and its mutants at 60 ℃ and pH 6.0

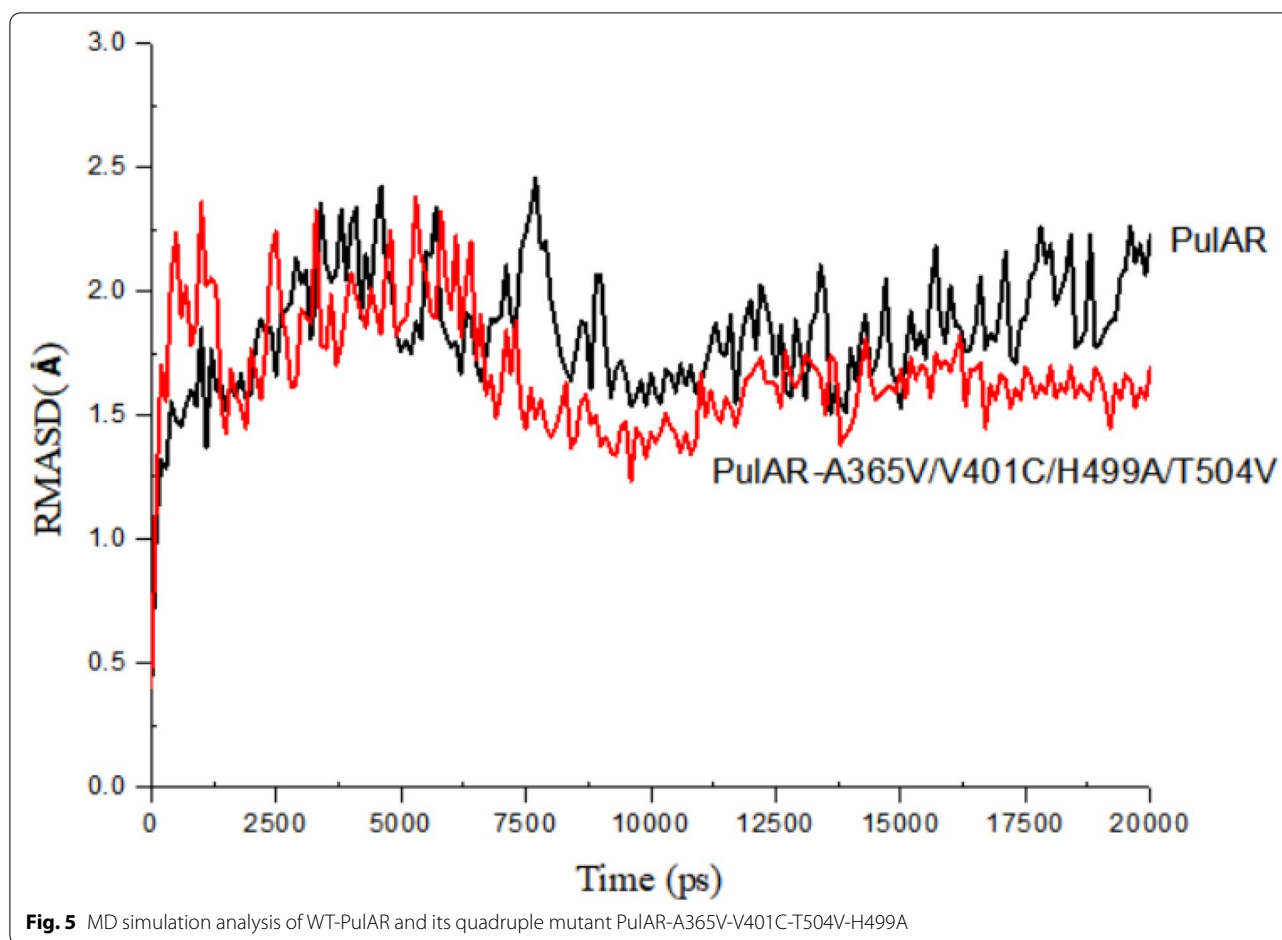| Mutant	v_{max} (μmol min^{-1} mg^{-1})	K_M (mg mL^{-1})	k_{cat} (s^{-1})	k_{cat}/K_M (mL mg^{-1} s^{-1})
WT-PulAR	31.6 ± 1.2	1.64 ± 0.20	52.7	32.1
PulAR-A365V	44.0 ± 2.3	1.52 ± 0.12	73.3	48.2
PulAR- V401C	48.8 ± 1.6	1.52 ± 0.50	81.3	54.2
PulAR-A365V-V401C	85.0 ± 2.5	1.24 ± 0.32	141.7	114.3
PulAR-A365V-V401C-T504V	92.9 ± 2.0	1.09 ± 0.11	154.8	142.0
PulAR-A365V-V401C-T504V-H499A	112.0 ± 3.1	0.77 ± 0.15	186.7	242.5

Table 5 Catalytic efficiencies of WT-PulAR and its mutants at 60 ℃ and pH 5.0

Mutant	v_{max} (μmol min^{-1} mg^{-1})	K_M (mg mL^{-1})	k_{cat} (s^{-1})	k_{cat}/K_M (mL mg^{-1} s^{-1})
WT-PulAR	25.6 ± 1.1	4.67 ± 0.12	42.7	9.1
PulAR-A365V	35.3 ± 0.3	3.96 ± 0.13	58.8	14.8
PulAR-V401C	37.3 ± 0.5	3.77 ± 0.20	62.2	16.8
PulAR-A365V-V401C	65.3 ± 1.2	3.19 ± 0.50	108.8	34.1
PulAR-A365V-V401C-T504V	76.0 ± 2.3	2.63 ± 0.28	126.7	48.2
PulAR-A365V-V401C-T504V-H499A	84.7 ± 1.6	1.47 ± 0.05	141.2	96.1

and D554. And all the single mutation A365V, V401C, T504V, H499, and the superposition of mutations tends to confer increased flexibility of the active sites, resulting in the increased catalytic efficiencies (Tables 4, 5).

To further investigate the mechanism of the PulAR mutant against high temperature and acidic pH, MD simulation analysis of PulAR and the quadruple mutant PulAR-A365V-V401C-T504V-H499A was conducted. As shown in Fig. 5, during the initial 6 ns for simulation, both the structures of PulAR and quadruple mutant PulAR-A365V-V401C-T504V-H499A are unstable. The entire protein conformation of the quadruple mutant

Li *et al. Bioresources and Bioprocessing*　　(2022) 9:25

Page 10 of 11

Fig. 5 MD simulation analysis of WT-PulAR and its quadruple mutant PulAR-A365V-V401C-T504V-H499A

became more stable than PulAR after 6 ns simulation time, which was consistent with stability enhancement under the thermophilic and acidic conditions.

In this work, the catalytic performance of PulAR under the thermophilic and acidic conditions was significantly enhanced by using a structure-guided consensus approach. Four mutations A365V, V401C, T504V, and H499A were obtained by SDM. Finally, the "best" quadruple mutant PulAR-A365V/V401C/T504V/H499A showed higher catalytic activity and thermostabilities under the thermophilic and acidic conditions. Structural comparison indicated that the increased internal hydrophobic interactions, the reduced solvent accessibility surface area and the increased hydrophilic of the protein surface are the main reasons for the enhancement of thermostability and acid resistance. The "best" mutant PulAR-A365V/V401C/T504V/H499A exhibited great potential in the production of high-purity maltose syrup and other related starch processing industry.

Supplementary Information

The online version contains supplementary material available at https://doi.org/10.1186/s40643-022-00516-4.

Additional file 1: Table S1. Primers design for site-directed mutagenesis. **Table S2.** Activity ratios of PulAR and its mutants at pH 5.0 to at pH 6.0. **Fig. S1.** SDS-PAGE analysis of WT-PulA and its mutants. M, Markers; Lane 1, purified WT-PulA; Lane 2, purified PulA-A365V; Lane 3, purified PulA-V401C; Lane 4, purified PulA-A365V/V401C; Lane 5, purified PulA-A365V/V401C/T504C; Lane 6, purified PulA-A365V/V401C/T504C/H499A. **Fig. S2.** Multiple sequence alignment of pullulanases from *Anoxybacillus* sp. AR-29, *Anoxybacillus* sp. LM18-11, *Bacillus acidopullulyticus* and *Bacillus naganoensis*. Conserved residues are indicated in frames.

Authors' contributions
YJW conceived of the study. SFL performed the experiment. SFL and SYX statistically analyzed the data, and collected the data. YJW and SYX drafted the manuscript. YGZ revised the manuscript. All authors read and approved the final manuscript.

Li *et al. Bioresources and Bioprocessing*   (2022) 9:25

Page 11 of 11

Declarations

Ethics approval and consent to participate
Not applicable.

Consent for publication
All the authors have read and approved to submit it to *Bioresources and Bioprocessing*.

Competing interests
The authors declare no competing financial interests.

Author details
[1]Key Laboratory of Bioorganic Synthesis of Zhejiang Province, College of Biotechnology and Bioengineering, Zhejiang University of Technology, 18 Chaowang Road, Hangzhou 310014, People's Republic of China. [2]Engineering Research Center of Bioconversion and Biopurification of the Ministry of Education, Zhejiang University of Technology, Hangzhou, Zhejiang 310014, People's Republic of China. [3]The National and Local Joint Engineering Research Center for Biomanufacturing of Chiral Chemicals, Zhejiang University of Technology, Hangzhou 310014, People's Republic of China.

References
Albertson GD, McHale RH, Gibbs MD, Bergquist PL (1997) Cloning and sequence of a type I pullulanase from an extremely thermophilic anaerobic bacterium, *Caldicellulosiruptor saccharolyticus*. Biochim Biophys Acta Gene Struct Express 1354(1):35–39

Bertoldo C, Antranikian G (2002) Starch-hydrolyzing enzymes from thermophilic archaea and bacteria. Curr Opin Chem Biol 6(2):151–160

Bertoldo C, Duffner F, Jorgensen PL, Antranikian G (1999) Pullulanase type I from *Fervidobacterium pennavorans* Ven5: cloning, sequencing, and expression of the gene and biochemical characterization of the recombinant enzyme. Appl Environ Microbiol 65(5):2084–2091

Bertoldo C, Armbrecht M, Becker F, Schäfer T, Antranikian G, Liebl W (2004) Cloning, sequencing, and characterization of a heat- and alkali-stable type I pullulanase from *Anaerobranca gottschalkii*. Appl Environ Microbiol 70(6):3407–3416

Bi J, Chen S, Zhao X, Nie Y, Xu Y (2020) Computation-aided engineering of starch-debranching pullulanase from *Bacillus thermoleovorans* for enhanced thermostability. Appl Microbiol Biotechnol 104(17):7551–7562

Böttcher D, Bornscheuer UT (2010) Protein engineering of microbial enzymes. Curr Opin Microbiol 13(3):274–282

Chen A, Xu T, Ge Y, Wang L, Tang W, Li S (2019) Hydrogen-bond-based protein engineering for the acidic adaptation of *Bacillus acidopullulyticus* pullulanase. Enzyme Microb Technol 124:79–83

Duan X, Chen J, Wu J (2013) Improving the thermostability and catalytic efficiency of *Bacillus deramificans* pullulanase by site-directed mutagenesis. Appl Environ Microbiol 79(13):4072–4077

Hii SL, Tan JS, Ling TC, Ariff AB (2012) Pullulanase: role in starch hydrolysis and potential industrial applications. Enzyme Res 2012:921362

Kahar UM, Ng CL, Chan KG, Goh KM (2016) Characterization of a type I pullulanase from *Anoxybacillus* sp. SK3–4 reveals an unusual substrate hydrolysis. Appl Microbiol Biotechnol 100(14):6291–6307

Kang J, Park KM, Choi KH, Park CS, Kim GE, Kim D, Cha J (2011) Molecular cloning and biochemical characterization of a heat-stable type I pullulanase from *Thermotoga neapolitana*. Enzyme Microb Technol 48(3):260–266

Kuriki T, Park JH, Imanaka T (1990) Characteristics of thermostable pullulanase from *Bacillus stearothermophilus* and the nucleotide sequence of the gene. J Ferment Bioeng 69(4):204–210

Li WF, Zhou XX, Lu P (2005) Structural features of thermozymes. Biotechnol Adv 23(4):271–281

Li Y, Zhang L, Niu D, Wang Z, Shi G (2012) Cloning, expression, characterization, and biocatalytic investigation of a novel bacilli thermostable type I pullulanase from *Bacillus* sp. CICIM 263. J Agric Food Chem 60(44):11164–11172

Li SF, Xu JY, Bao YJ, Zheng HC, Song H (2015) Structure and sequence analysis-based engineering of pullulanase from *Anoxybacillus* sp. LM18-11 for improved thermostability. J Biotechnol 210:8–14

Li L, Dong F, Lin L, He D, Wei W, Wei D (2018) N-terminal domain truncation and domain insertion-based engineering of a novel thermostable type I pullulanase from *Geobacillus thermocatenulatus*. J Agric Food Chem 66(41):10788–10798

Lin Q, Xiao H, Liu GQ, Liu Z, Li L, Yu F (2013) Production of maltose syrup by enzymatic conversion of rice starch. Food Bioprocess Technol 6(1):242–248

Nie Y, Yan W, Xu Y, Chen WB, Mu XQ, Wang X, Xiao R (2013) High-level expression of *Bacillus naganoensis* pullulanase from recombinant *Escherichia coli* with auto-induction: effect of lac operator. PLoS ONE 8(10):e78416

Pang B, Zhou L, Cui W, Liu Z, Zhou S, Xu J, Zhou Z (2019) A hyperthermostable type II pullulanase from a deep-sea microorganism *Pyrococcus yayanosii* CH1. J Agric Food Chem 67(34):9611–9617

Tai H, Irie K, Mikami SI, Yamamoto Y (2011) Enhancement of the thermostability of hydrogenobacter thermophilus Cytochrome c552 through introduction of an extra methylene group into its hydrophobic protein interior. Biochemistry 50(15):3161–3169

Turkenburg JP, Brzozowski AM, Svendsen A, Borchert TV, Davies GJ, Wilson KS (2009) Structure of a pullulanase from *Bacillus acidopullulyticus*. Proteins 76(2):516–519

Wang QY, Xie NZ, Du QS, Qin Y, Li JX, Meng JZ, Huang RB (2017) Active hydrogen bond network (AHBN) and applications for improvement of thermal stability and pH-sensitivity of pullulanase from *Bacillus naganoensis*. PLoS ONE 12(1):e0169080

Wei W, Ma J, Chen SQ, Cai XH, Wei DZ (2015) A novel cold-adapted type I pullulanase of *Paenibacillus polymyxa* Nws-pp2: in vivo functional expression and biochemical characterization of glucans hydrolyzates analysis. BMC Biotechnol 15:96

Xu J, Ren F, Huang CH, Zheng Y, Zhen J, Sun H, Ko TP, He M, Chen CC, Chan HC, Guo RT, Song H, Ma Y (2014) Functional and structural studies of pullulanase from *Anoxybacillus* sp. LM18–11. Proteins 82(9):1685–1693

Yang S, Yan Q, Bao Q, Liu J, Jiang Z (2017) Expression and biochemical characterization of a novel type I pullulanase from *Bacillus megaterium*. Biotechnol Lett 39(3):397–405

Yang Y, Zhu Y, Obaroakpo JU, Zhang S, Lu J, Yang L, Ni D, Pang X, Lv J (2020) Identification of a novel type I pullulanase from *Fervidobacterium nodosum* Rt17-B1, with high thermostability and suitable optimal pH. Int J Biol Macromol 143:424–433

Yu XW, Wang R, Zhang M, Xu Y, Xiao R (2012) Enhanced thermostability of a Rhizopus chinensis lipase by in vivo recombination in Pichia pastoris. Microb Cell Fact 11:102

Zeng Y, Xu J, Fu X, Tan M, Liu F, Zheng H, Song H (2019) Effects of different carbohydrate-binding modules on the enzymatic properties of pullulanase. Int J Biol Macromol 137:973–981

Zhang SY, Guo ZW, Wu XL, Ou XY, Zong MH, Lou WY (2020) Recombinant expression and characterization of a novel cold-adapted type I pullulanase for efficient amylopectin hydrolysis. J Biotechnol 313:39–47

Zouari Ayadi D, Ben Ali M, Jemli S, Ben Mabrouk S, Mezghani M, Ben Messaoud E, Bejar S (2008) Heterologous expression, secretion and characterization of the *Geobacillus thermoleovorans* US105 type I pullulanase. Appl Microbiol Biotechnol 78(3):473–481

Publisher's Note
Springer Nature remains neutral with regard to jurisdictional claims in published maps and institutional affiliations.